

# A COMPARATIVE STUDY OF THE IMPULSIVE NOISE REDUCTION ALGORITHMS IN ULTRASONIC B-SCANS

Ramon Miralles, Raquel Molina

Instituto de Telecomunicaciones y Aplicaciones Multimedia (iTEAM)  
 Universidad Politécnica de Valencia, Camino de Vera S/N, 46022, Valencia, Spain  
 phone: +3496 3879737, fax: +3496 3877309, email: rmiralle@dcom.upv.es, web: www.gts.upv.es

## ABSTRACT

As the technology becomes cheaper and industries are conscious of the quality control importance, ultrasonic inspection becomes more popular. However, automatic inspection systems instead of manual ones should be designed if a successful implantation is desired. Signal processing algorithms play an important role on the designing of these systems. Unfriendly environment found in production lines cause that these systems should make intensive use of noise reduction algorithms. This work deals with studying the best algorithm for impulsive noise reduction in an industrial environment. A review of the typical impulsive noise reduction systems is done and particularized for the described situation. Finally, computational aspects are analyzed and some solutions are proposed.

## 1. INTRODUCTION

In industrial applications of non-destructive testing using ultrasounds is very frequent to find alternating current (AC) motors. These AC motors are commonly running in the vicinity of non-destructive testing equipment and are used for example for operating transport belts. The rotational speed of this engines is controlled by the Variable Frequency Drive (VFD). The VFD is a nonlinear device that introduces a large amount of noise that is picked up by the ultrasonic receiver electronics difficulting the flaw detection. In some situations the noise presence could be minimized with a good hardware and shielding design. However there are other situations where it is not possible to make such a design, for instance impossibility to use relatively short cables between the transducer and the ultrasonic pulser/ receiver. In this situations, signal processing algorithms can help to remove the impulsive noise and facilitate the design of the defect detector. Additionally, it has to be taken into account the need of real time algorithms in industrial systems. Production lines work fast and the distance from product to product is in most of the situations a few centimeters, so that fast algorithms should be employed. In this work different algorithms for reducing the impulsive noise in the ultrasonic B-scans will be analyzed. The work will be structured as follows. In the next section we will study and model the noise. Later in section 3 different signal processing algorithms for reducing this noise will be proposed. In section 4 the presented algorithms will be tested in a simulated scenario (subsection 4.1) and finally in subsection 4.2 real examples will be shown. The work finishes with some conclusions.

This work was supported by the national R+D program under grant TEC2008-02975 (Spain) and FEDER programme.

## 2. ON THE MODELLING OF IMPULSIVE NOISE IN A TRAVELLING BELT SCENARIO

Lets assume that we are doing an ultrasonic inspection of a material that is travelling on a transport belt of a production line. The ultrasonic transducer somehow fixed to the production line. We will assume that the coupling of the transducer to the inspected material is somewhat solved. We will assume also that material geometry allows doing this kind of inspection. If the ultrasonic transducer works in pulse-echo mode, B-scans are obtained. B-scans are defined as a successive number of captured A-scans (ultrasonic traces) for different positions. The following experiment was done to measure and model the effect of the ultrasonic noise in the B-scans as a consequence of the alternating current engine.

A polyethylene rectangular box filled with distilled water was placed on the transport belt of the production line. Different B-scans were acquired for different rotational speeds of the engines. The rotational speed was controlled varying the frequency of the VFD. The VFD generates Electro Magnetic Interferences (EMI) that couple into the receiver electronics contaminating the B-scan in form of impulsive noise. The ultrasonic B-scans acquired with this experiment resemble a noisy background with a unique ultrasonic echo due to the reflection on the top of the water tank (see figure 1). This experiment was repeated for different frequencies of the VFD in the range  $f_{VFD} = \{0Hz - 50Hz\}$ . This analysis allows to study the impulsive noise statistics. The figure 2 shows the measured probability density function of the coupled noise at the different speeds. The results obtained are similar to what some other authors have measured [1].

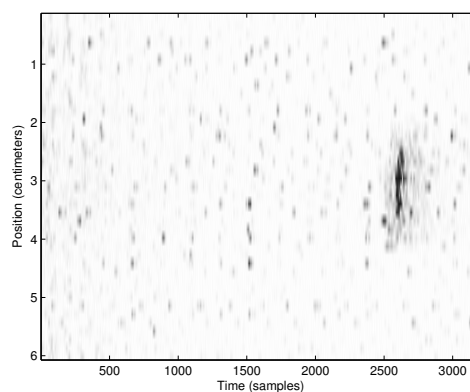


Figure 1: An acquired ultrasonic B-scan with impulsive noise (only the backwall echo should be visible).

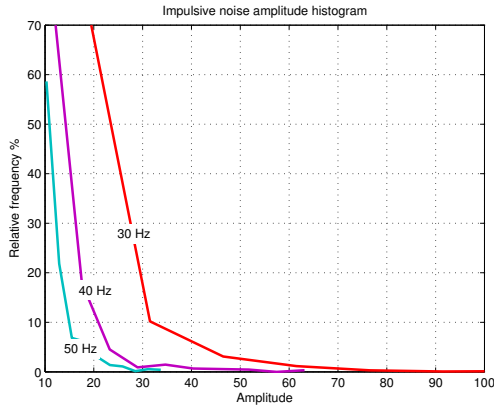


Figure 2: Estimated probability density function of the impulsive noise amplitude at different speeds of the VFD.

The empirically estimated distributions resemble an exponential distribution for the impulsive noise. A Kolmogorov-Smirnov test [2] was performed to compare impulsive noise with exponential distribution. The null hypothesis was that the measured noise statistics have the expected distributions. The null hypothesis is accepted at the 95 % of significance. It is interesting to observe in the figure 2 that the impulsive noise amplitudes are not directly proportional to the VFD frequency. A possible justification is based on the fact that VFDs are nonlinear devices with an input frequency of 50 Hz from the power line. The amount of non-linearity that the VFD has to introduce to achieve a target frequency depends on how far this frequency is from the natural frequency (50 Hz). The number of impulses were also measured (see table 1).

Frequency :	30 Hz	40 Hz	50 Hz
Number of pulses :	4186	1460	885

Table 1: Number of impulses measured for different frequencies of the VFD (different travelling belt speeds).

### 3. IMPULSIVE NOISE REDUCTION ALGORITHMS

A bibliographic review of the different methods employed to remove impulsive noise in images was done. The standard median filter [3], the weighted median filter [4, 5] and decision based median filter [6, 7] were frequently found. All this variants try to deal with the problem that median filters remove very well isolated noise preserving sharp edges but destroys small edges altering natural information. An interesting alternative to the nonlinear median filtering can be found in [8]. This alternative, also called the peak-and-valley filter, is much faster than the median filter and gives comparable results in terms of percentage of eliminated noise in typical image processing applications [8]. Also, it is worth mentioning the Savitzky-Golay filters. According to [9], filters based on these polynomials can be developed and they achieved comparable level of noise reduction and similar edge preservation on ultrasonic signals with considerably less computation time. The fundamental idea of these filters is to fit a different polynomial to the data surrounding each data point.

The smoothed points are computed by replacing each data point with the value of its fitted polynomial. The interesting part is that the polynomial coefficients can be computed with a linear filter. For smoothing, only one coefficient of the polynomial is needed, so the whole process of least squares fitting at every point becomes a simple process of applying the appropriate linear filter at every point [9].

The designed algorithm should fulfill the following requirements: reduce impulsive noise, preserve sharp edges like those appearing in the B-scan due to large impedance changes in the propagation of the ultrasonic signal (backwall echo) and preserve small edges like those due to flaws, defects, foreign bodies, etc. Additionally, low computational cost was taken into account to implement a system working in real time. The noise reduction algorithms were selected from the bibliography and adjusted to behave as previously described. The following Noise Reduction Algorithms (NRA) were tested:

1. Standard median filter: 2-D median filtering of the ultrasonic B-scan with a 3x3 window.
2. Decision based median filter: 2-D median filtering of the ultrasonic B-scan with a 3x3 window only for those pixels satisfying the condition described in equation (1). The algorithm was implemented as described in [7].

$$Threshold = \min \left[ \frac{|b(i,j) - m_H|}{\sigma_H + 1}, \frac{|b(i,j) - m_V|}{\sigma_V + 1} \right] \quad (1)$$

The value of the B-scan at the particular pixel is given by  $b(i, j)$ . The values  $m_H, m_V / \sigma_H, \sigma_V$  are the median and standard deviation in the horizontal (1x3) / vertical (3x1) windows around  $b(i, j)$ .

3. Column-wise standard median filter: A 1-D standard median filter of order 3 operating on each column of the B-scan.
4. Peak-and-valley filter: A 2-D filter as described in [8].
5. Row-wise Savitzky-Golay filter: A 1-D Savitzky-Golay filter operating on each A-scan (rows of the B-scan). A polynomial of order 3 and a frame size of 100 was employed.

The window size employed in the median algorithms and the order of the Savitzky-Golay polynomial were chosen empirically. The selected value should satisfy the condition that small gradual echoes from foreign bodies were preserved.

## 4. RESULTS

### 4.1 Simulation study on synthetic B-scans

Envelope of the ultrasonic B-scans was modeled by discrete 2-D convolution of the binary image ( $\mathbf{X}$ ) shown in figure 3 with a 2-D Gaussian matrix ( $\mathbf{H}$ ) as described in equation (2). The 2-D matrix ( $\mathbf{X}$ ) models the reflections: backwall or defect reflection for instance. The matrix  $\mathbf{H}$  models the 2-D Gaussian envelope of an isolated ultrasonic pulse [10]. Matrix  $\mathbf{H}$  was generated using equation (3) with  $\sigma_i = 10$ ,  $\sigma_j = 1 \cdot 10^{-1}$  and  $(i, j)$  being in the range of  $\{-20, \dots, -20\}$ . We will assume that the result of the convolution is a matrix of size  $M \times N$ .

$$\mathbf{B} = \mathbf{X} * \mathbf{H} \quad (2)$$

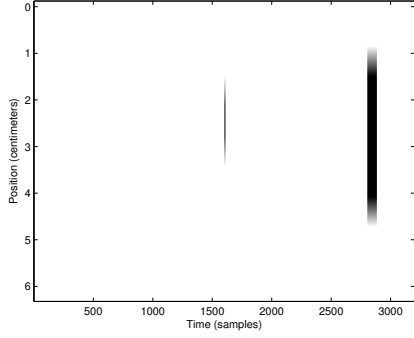


Figure 3: Synthetic binary B-scan ( $\mathbf{X}$  matrix).

$$\mathbf{H} = h(i, j) = e^{-\left(\frac{i^2}{2\sigma_i^2} + \frac{j^2}{2\sigma_j^2}\right)} \quad (3)$$

$$\mathbf{N} = N(\tilde{i}, \tilde{j}) = \tilde{\phi} \quad (4)$$

$$\mathbf{B}_n = \mathbf{B} + \mathbf{N} \quad (5)$$

$$\mathbf{B}_{nf} = NRA[\mathbf{B} + \mathbf{N}] \quad (6)$$

After obtaining the synthetic B-scan, impulsive noise matrix ( $\mathbf{N}$ ) was generated according to equation (4). The integer random variables  $\tilde{i}$  and  $\tilde{j}$  were uniformly distributed in the range  $\{0, \dots, M-1\}$  for  $\tilde{i}$ , and  $\{0, \dots, N-1\}$  for  $\tilde{j}$ . The continuous random variable  $\tilde{\phi}$  was exponential distributed as it was measured to be in the experiment described in section 2. Finally, the matrices  $\mathbf{B}$  and  $\mathbf{N}$  were added according to equation (5) and filtered with the five proposed NRAs (see equation (6)). An illustrative result for standard median filter algorithm can be seen in the figure 4.

The different noise reduction algorithms were tested on the synthetic B-scans with the number of impulses changing in the measured range (table 1). In order to compare the performance, the Signal to Noise Ratio (SNR) was calculated. The Signal was taken to be the energy of the simulated scenario: the possible defect and backwall echo (numerator in equation (7)). This term will be of interest for a posteriori detection of the possible flaw. The remaining noise was computed after filtering with each one of the proposed algorithms. The SNR was finally computed as follows:

$$SNR = \frac{\sum_i \sum_j B^2(i, j)}{\sum_i \sum_j (B(i, j) - B_{nf}(i, j))^2} \quad (7)$$

The figure 5 shows the SNR in dB, as described in equation (7), for all the tested algorithms when the number of impulses increases. The figure shows that decision based median filter and standard median filter achieve the highest noise reduction ratio in all conditions of impulsive noise. In situations where a large amount of EMI (equivalently impulsive noise) is present the differences between the studied NRAs become lower. In all cases the peak-and-valley algorithm show to be not very effective removing impulsive noise in the simulated scenario.

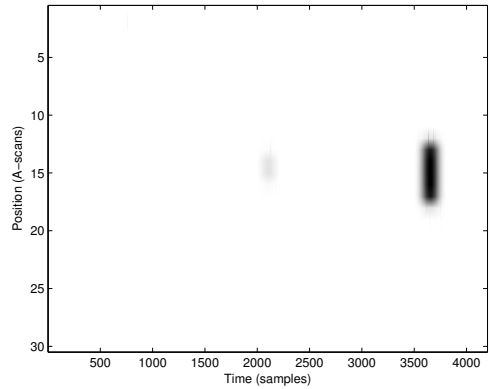
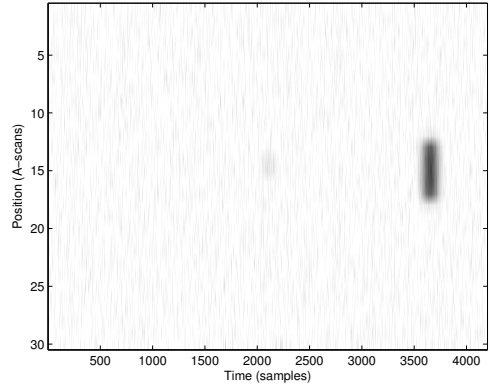


Figure 4: An example of a synthetic B-scan with impulsive noise and after processing with the standard median filter.

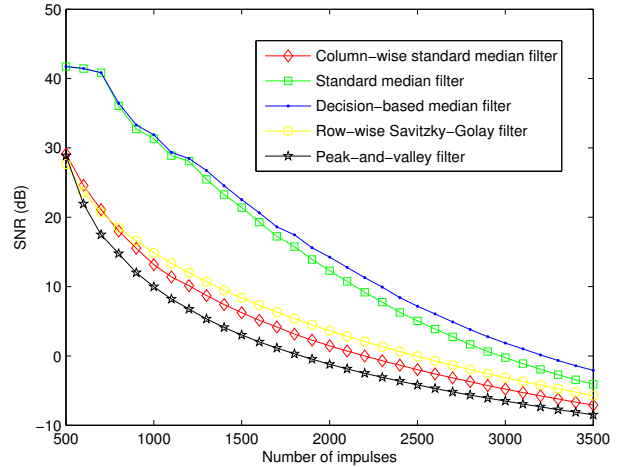


Figure 5: SNR (dB) evolution when the number of EMI impulses increases for the proposed NRAs.

At this point we are going to analyze the computational complexity of each proposed algorithm. Taking into account that the B-scan is a  $M \times N$  matrix and using a typical sorting algorithm with good performance, the computational com-

plexity in terms of the size list  $K$  is  $\mathcal{O}(K \cdot \log(K))$  [11]. Using this result, we can derive the computational complexity for the proposed algorithms as shown in table 2. The size list  $K$  in the table 2 should be set to  $K = 3$  for the particular NRA described in the section 3. The additional parameter  $\rho$  that appears for decision based median filters (table 2) depends on the noise statistics and density of impulses. This value will be close to 1 in high density impulsive noise scenarios and tries to model that due to the decision rule not all medians should be computed reducing computational complexity. In the case of the Savitzky-Golay filter the process of the least-squares fits would be laborious since it involves a linear matrix inversion. Fortunately, we can do the fitting in advance for fictitious data and then do the fits on the real data just by taking linear combinations [12]. As a result of that, the process of filtering using the Savitzky-Golay filter has the same complexity as using a simple FIR filter (see table 2).

Algorithm :	Computational Complexity
Standard median :	$M \cdot N \cdot \mathcal{O}(K^2 \log K^2)$
Decision median :	$M \cdot N \cdot (\mathcal{O}(K^2 \log K^2) \rho + \mathcal{O}(2 \cdot K))$
Column median :	$M \cdot N \cdot \mathcal{O}(K \log K)$
Peak-and-valley :	$M \cdot N \cdot \mathcal{O}(K^2)$
Savitzky-Golay :	$M \cdot \mathcal{O}(N \log N)$ <sup>1</sup>

Table 2: Computational complexity of the different algorithms ( $K = 3$  for the NRA presented).

From the results presented in the table 2 can be derived that the fastest algorithm is the column-wise median filter followed by the Savitzky-Golay filter. The peak-and-valley algorithm is computationally less complex than the standard median filter and the decision based median filter.

#### 4.2 On the processing of real B-scans

The experiment described in section 2 was repeated but this time a 5 mm stainless steel piece of metal was introduced in the water tank. The foreign body was held by a 0.1 mm of diameter nylon line in order to keep it at a constant depth. The ultrasonic B-scan was acquired with the VFD working at 30 Hz. The figure 7 shows the original B-scan as well as the processed B-scans with some of the presented noise reduction algorithms. The figure presents results only for the decision based median algorithm, the column-wise standard median filter and the Savitzky-Golay filter. The results with the standard median filter were very similar to the decision based median filter and have been omitted. As it was predicted in the simulations the peak and valley algorithm gave the worst results when denoising ultrasonic B-scans under the conditions established. It is interesting to observe that the results with the column-wise median filter are almost as good as the results with decision-based median algorithm. A zoomed region of the the B-scan is shown in the figure 7 with an optimized palette to bring out the differences. In the zoomed region it can be observed that the decision based algorithm performs better than the column-wise. However, differences were not as big as expected. A possible explanation of this result is based on the fact that measured impul-

<sup>1</sup>We have assumed that the convolution has been done using Fast Fourier Transform

sive noise present some degree of correlation in the temporal dimension of the B-scan and no correlation in the spatial dimension. The impulsive noise simulated did not present correlation in any of the dimensions.

### 5. CONCLUSIONS AND FUTURE LINES

This work shows how typical impulsive noise reduction algorithms can be used with excellent results to reduce the noise produced by EMI interferences in the ultrasonic flaw detection problem. Performance in terms of eliminated noise per computational complexity, varies among the algorithms. If real time operation of the algorithms becomes a restriction not all the studied techniques are equally valid.

The peak-and-valley algorithm gave the worst results in terms of SNR on the simulated and real scenarios.

The Savitzky-Golay and the Column-wise median algorithms gave poor results in simulated B-scans. However, the Column-wise algorithm gave good results in real B-scans. This fact, alongside the low computational cost suggests using Column-wise algorithm for real time impulsive noise reduction in ultrasonic B-scans.

The decision-based median filter gave the best results, in terms of SNR, on simulated B-scans. However, when it was applied to real B-scans results were worse than expected. An explanation of this result is based on the fact that measured impulsive noise present some degree of correlation in the temporal dimension of the B-scan and no correlation in the spatial dimension. The impulsive noise simulated did not present correlation in any of the dimensions.

A possible future research line consists of using the obtained information of the impulsive noise statistics to design variants of median filters tailored to exploit this knowledge.

### REFERENCES

- [1] W. Henkel and T. Kessler. A simplified impulse-noise model for the xDSL test environment. October 1999.
- [2] D.J. Sheskin. *Handbook of Parametric and Nonparametric Statistical Procedures*. Chapman and Hall CRC, 4 edition, 2007.
- [3] I. Pitas and A.N. Venetsanopoulos. *Nonlinear digital filters: principles and applications*. Kluwer, 1990.
- [4] T. Loupass, W.N. McDicken, and P.L. Allan. An adaptive weighted median filter for speckle suppression in medical ultrasonic images. *IEEE Transactions on Circuits and Systems*, 36:129–135, 1989.
- [5] P. Yang and O.A. Basir. Adaptive weighted median filter using local entropy for ultrasonic image de-noising. *Proceedings of the 3rd International Symposium on Image and Signal Processing and Analysis, Rome, Italy*, pages 799 – 803, 2003.
- [6] H. Parsiani. Isolated noise detection and reduction in color images. *Proceedings of the 36th Midwest Symposium on Circuits and System*, 36(1):16–18, August 1993.
- [7] D.A.F. Florencio and R.W. Schafer. Decision-based median filter using local signal statistics. *Proceedings of SPIE*, 2308:269 – 275, 1994.
- [8] P.S. Windyga. Fast impulsive noise removal. *IEEE Transactions on Image Processing*, 10(1):173 – 179, 2001.

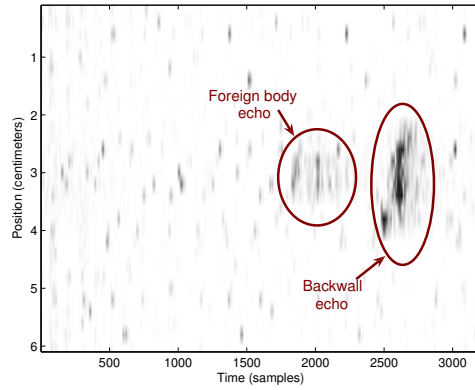


Figure 6: Original B-scan previous to processing with the proposed NRAs.

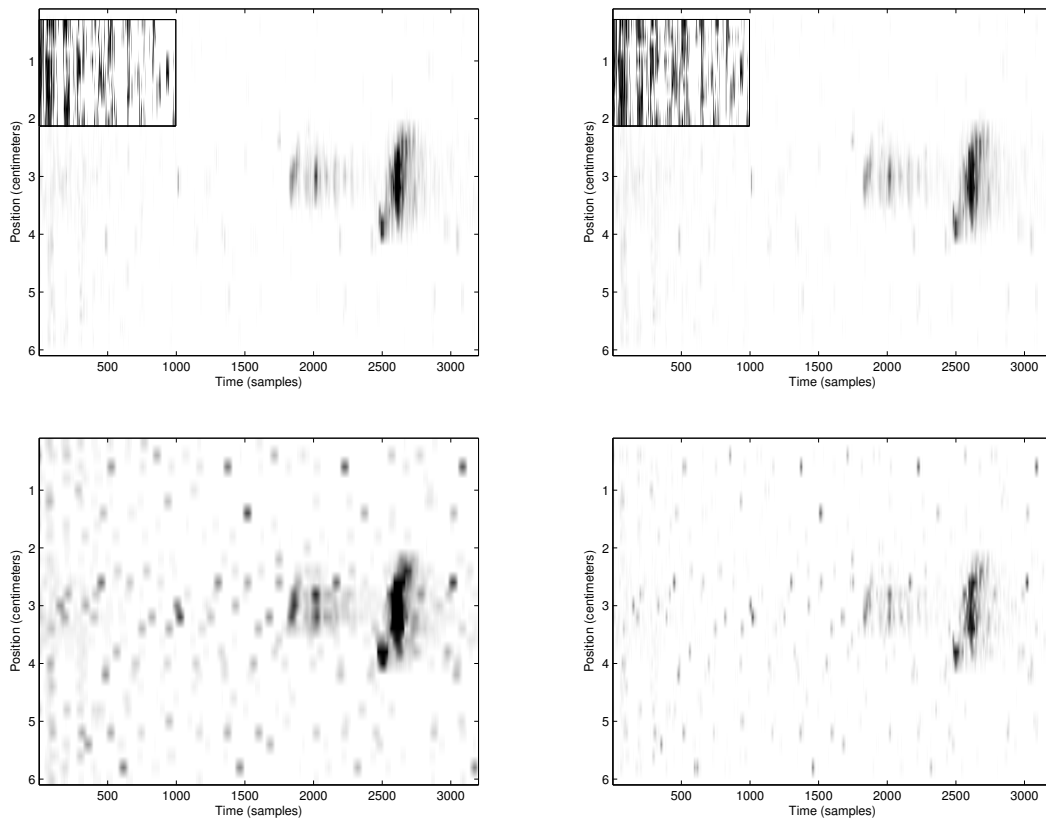


Figure 7: From top left to down right: processed with the decision based median filter, processed with the column-wise standard median filter, processed with the Savitzky-Golay filter and processed with the peak and valley filter. A small region of the B-scans is shown with a different colormap to bring out the differences.

- [9] C. Chinrungrueng and A. Suvichakorn. Fast edge-preserving noise reduction for ultrasound images. *IEEE Transactions on Nuclear Science*, 48(3):849 – 854, 2001.
- [10] R. Demirli and J. Saniie. Model-based estimation of ultrasonic echoes part i: Analysis and algorithms. *IEEE transactions on ultrasonics, ferroelectrics, and frequency control*, 48(3):787–802, May 2001.
- [11] D.E. Knuth. The art of computer programming, volume 3: Sorting and searching.
- [12] W.H. Press, S.A. Teukolsky, W.T. Vetterling, and B.P. Flannery. Numerical recipes in fortran 77: The art of scientific computing.